PHYSICAL REVIEW D, VOLUME 70, 096001

Branon search in hadronic colliders

J. A. R. Cembranos,[1,2] A. Dobado,[2] and A. L. Maroto[2]

[1]*Departamento de Estadística e Investigación Operativa III, Universidad Complutense de Madrid, 28040 Madrid, Spain*

[2]*Departamento de Física Teórica, Universidad Complutense de Madrid, 28040 Madrid, Spain*

(Received 8 June 2004; published 4 November 2004)

In the context of the brane-world scenarios with compactified extra dimensions, we study the production of brane fluctuations (branons) in hadron colliders ($p\bar{p}$, pp, and $e^{\pm}p$) in terms of the brane tension parameter f, the branon mass M, and the number of branons N. From the absence of monojet events at HERA and Tevatron (run I), we set bounds on these parameters and we also study how such bounds could be improved at Tevatron (run II) and the future LHC. The single-photon channel is also analyzed for the two last colliders.

DOI: 10.1103/PhysRevD.70.096001 PACS numbers: 11.25.Wx, 11.10.Lm, 11.15.Ex, 11.25.Mj

I. INTRODUCTION

Since rigid objects do not exist in relativistic theories, it is clear that brane fluctuations must play a role in the so-called brane world, proposed some years ago by Arkani-Hamed, Dimopoulos, and Dvali (ADD scenarios [1]), where the standard model (SM) particles are confined to live in the world brane and only gravitons are free to move along the $D > 4$ dimensional bulk space (see [2] for recent reviews). This fact turns out to be particularly true when the brane tension scale f ($\tau = f^4$ being the brane tension) is much smaller than the D dimensional or fundamental gravitational scale M_D, i.e., $f \ll M_D$. In this case the only relevant low-energy modes of the ADD scenarios are the SM particles and branons which are the quantized brane oscillations. Branons can be understood as the (pseudo)Goldstone bosons corresponding to the spontaneous breaking of translational invariance in the bulk space produced by the presence of the brane. It has been pointed out that branons could solve some of the problems of the brane-world scenarios such as the divergent virtual contributions from the Kaluza-Klein (KK) tower at the tree level or nonunitarity of the graviton production cross sections [3]. As Goldstone bosons, branons are in principle massless but, in the cases where the metric of the extra dimensions cannot be factorized, they can become massive [4,5]. This is similar to the case of pions which, being the Goldstone bosons of the spontaneous breaking of chiral symmetry, acquire some mass due to the explicit breaking of the symmetry induced by the quark masses.

In previous works, the different effective actions have been obtained; namely, the effective action for the SM fields on the brane, that for the branon self-interactions, and finally that corresponding to the interaction between SM fields and branons [4]. In general, this branon effective action can be parametrized by the number of branons N, the tension scale f, and the branon masses (for an explicit construction see [6]). Using the effective action it is possible to obtain the different Feynman rules, the amplitudes, and finally the cross sections for branon production from SM particles. In [7–9], the case of electron-positron colliders has been considered. By using the Large Electron-Positron Collider (LEP) data, it is possible to set important bounds on the tension scale and on the branon mass for a given branon number. Other restrictions have also been set from astrophysical and cosmological considerations due to the fact that branon dark matter can present relevant abundances [10].

In this work we study branon production in hadron colliders and also in electron-proton colliders such as HERA. Most of these cross sections have been studied by Creminelli and Strumia for the massless branon case [9]. We reproduce their results and extend the analysis for an arbitrary branon mass. The paper is organized as follows: In Sec. II we shortly review the branon effective action. In Sec. III we consider the case of proton-(anti)proton colliders like Tevatron or the future Large Hadron Collider (LHC). In Sec. IV electron(positron)-proton colliders like HERA are studied. In Sec. V we show the main results for the relevant examples and in Sec. VI we set the conclusions.

II. EFFECTIVE ACTION

The relevant effective action describing the low-energy interactions of SM particles and branons was derived in [7], where the necessary vertices are detailed. The branon effective action can be expanded according to the number of branon fields appearing in each term:

$$S_{\rm eff}[\pi] = S^{(0)}_{\rm eff}[\pi] + S^{(2)}_{\rm eff}[\pi] + \cdots, \tag{1}$$

where the zeroth-order term is just a constant and the second order is just the free action:

$$S^{(2)}_{\rm eff}[\pi] = \frac{1}{2}\int d^4x(\delta_{\alpha\beta}\partial_\mu\pi^\alpha\partial^\mu\pi^\beta - M^2_{\alpha\beta}\pi^\alpha\pi^\beta), \tag{2}$$

with $\pi^\alpha(x)$ the branon fields where $\alpha = 1, 2, \ldots, N$ and $M^2_{\alpha\beta}$ is the squared mass matrix which, without loss of generality, can be assumed to be diagonal. The effective action for the SM particles and their interactions with

branons is given by

$$S_{\mathrm{SM}\pi} = \int d^4x \Big[\mathcal{L}_{S\mathcal{M}} + \frac{1}{8f^4}(4\delta_{\alpha\beta}\partial_\mu\pi^\alpha\partial_\nu\pi^\beta - \eta_{\mu\nu}M^2_{\alpha\beta}\pi^\alpha\pi^\beta)T^{\mu\nu}_{\mathrm{SM}}\Big], \tag{3}$$

where $\mathcal{L}_{S\mathcal{M}}$ is the SM Lagrangian and $T^{\mu\nu}_{\mathrm{SM}}$ is the SM energy-momentum tensor defined as

$$T^{\mu\nu}_{\mathrm{SM}} = -\left(g^{\mu\nu}\mathcal{L}_{S\mathcal{M}} + 2\frac{\delta\mathcal{L}_{S\mathcal{M}}}{\delta g_{\mu\nu}}\right)\Big|_{g_{\mu\nu}=\eta_{\mu\nu}}, \tag{4}$$

where $g_{\mu\nu}$ is some arbitrary metric on the world brane and $\eta_{\mu\nu}$ is the Minkowski metric.

In this work we are interested in the interactions between quarks and gluons or photons. Thus, for Dirac fermions with masses m_q belonging to some representation of a gauge group, such as $U(1)_{em}$ or $\mathrm{SU}(3)_c$, with generators T^a, the Lagrangian is

$$\mathcal{L}_q = \bar{q}(i\gamma^\mu D_\mu - m_q)q, \tag{5}$$

where the covariant derivative is defined as $D_\mu = \partial_\mu - hA^a_\mu T^a$, h being the appropriate gauge coupling. Thus, the energy-momentum tensor is given by

$$T^{\mu\nu}_q = \frac{i}{4}[\bar{q}(\gamma^\mu D^\nu + \gamma^\nu D^\mu)q - (D^\nu\bar{q}\gamma^\mu + D^\mu\bar{q}\gamma^\nu)q] - \eta^{\mu\nu}[i(\bar{q}\gamma^\rho D^\rho - D_\rho\bar{q}\gamma^\rho)q - 2m_q\bar{q}q], \tag{6}$$

from where it is possible to find vertices such as $\pi\pi\bar{q}q$ and $\pi\pi\bar{q}qA$. For gauge fields A, the appropriate Lagrangian for perturbation theory is

$$\mathcal{L}_{\mathcal{A}} = -\tfrac{1}{4}F^{a\mu\nu}F^a_{\mu\nu} + \mathcal{L}_{\mathcal{FP}}, \tag{7}$$

where as usual $F^a_{\mu\nu} = \partial_\mu A^a_\nu - \partial_\nu A^a_\mu - hC^{abc}A^b_\mu A^c_\nu$ and $\mathcal{L}_{\mathcal{FP}}$ is the Fadeev-Popov Lagrangian including the gauge fixing and the ghost terms. The energy-momentum tensor is

$$T^{\mu\nu}_A = F^a_{\rho\sigma}F^a_{\lambda\theta}(\eta^{\sigma\lambda}\eta^{\rho\mu}\eta^{\theta\nu} + \tfrac{1}{4}\eta^{\rho\lambda}\eta^{\sigma\theta}\eta^{\mu\nu}) + T^{\mu\nu}_{FP}, \tag{8}$$

from where we can obtain the $\pi\pi AA$, $\pi\pi AAA$, and $\pi\pi AAAA$ vertices.

Therefore, by using these energy-momentum tensors and the effective action above, it is possible to obtain the different Feynman rules involving branons. One important observation is that, in all the vertices obtained above, branons appear always by pairs. In fact, they interact in a way similar to gravitons since they couple to the energy-momentum tensor. This can be seen by making the formal identification of the graviton field $h_{\mu\nu}$ which appears in linearized gravity with

$$h_{\mu\nu} \to -\frac{1}{\kappa f^4}\left(\delta_{\alpha\beta}\partial_\mu\pi^\alpha\partial_\nu\pi^\beta - \frac{1}{4}\eta_{\mu\nu}M_{\alpha\beta}\pi^\alpha\pi^\beta\right), \tag{9}$$

where $\kappa = 4\sqrt{\pi}/M_P$ and M_P is the Planck mass. Of course, the physical meaning is completely different for branons and gravitons. In any case, branons are expected to be weakly interacting and then they will escape from detection. Hence, their typical signature will be missing energy and momentum. Since branons are produced by pairs, the energy spectrum of any other particle present in the final state will be continuous. In the following sections, we will study the production mechanisms relevant for the different hadronic colliders.

III. PROTON-(ANTI)PROTON COLLIDERS

For the case of proton-antiproton colliders like Tevatron, the most important processes for branon production are quark-antiquark annihilation or gluon fusion giving a gluon and a branon pair, and (anti)quark-gluon interaction giving an (anti)quark and a branon pair. Therefore the expected experimental signal will be in both cases one monojet J and missing energy and momentum. This is a very clear signature that in principle can be easily identified. Another potentially interesting process is the quark-antiquark annihilation giving a photon and a branon pair. In this case, the signature is one single-photon and missing energy and momentum.

The Feynman diagrams contributing to the main subprocesses $q\bar{q} \to g\pi\pi$, $gg \to g\pi\pi$, $qg \to q\pi\pi$, $\bar{q}g \to \bar{q}\pi\pi$, and $q\bar{q} \to \gamma\pi\pi$ are shown in Figs. 1–4.

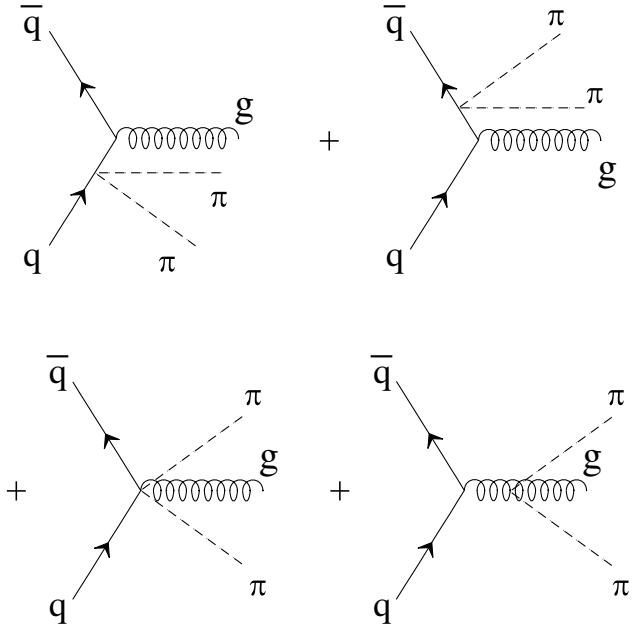

FIG. 1. Feynman diagrams associated with the $q\bar{q} \to g\pi\pi$ subprocess.

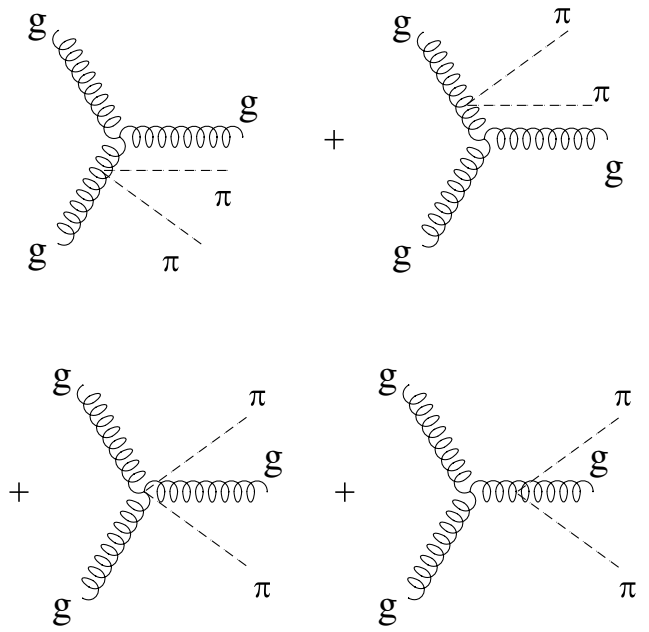

FIG. 2. Feynman diagrams associated with the $gg \to g\pi\pi$ subprocess.

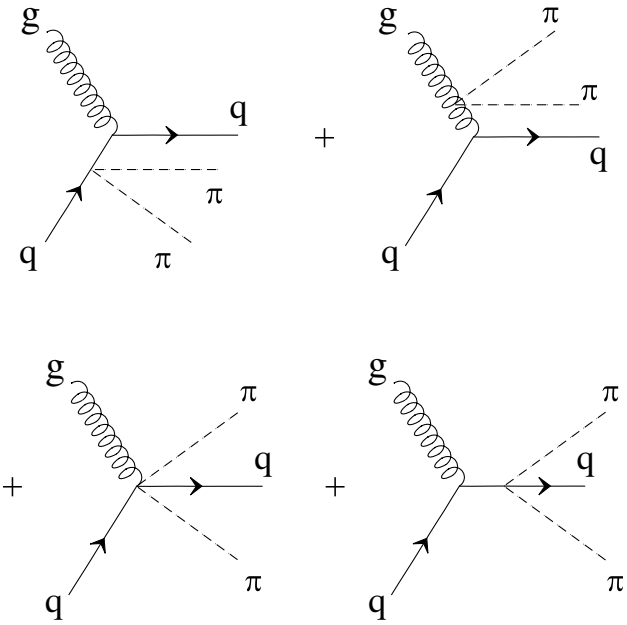

FIG. 3. Feynman diagrams associated with the $qg \to q\pi\pi$ subprocess. The $\bar{q}g \to \bar{q}\pi\pi$ subprocess has the same diagrams, but changes the quark lines by the corresponding antiquark ones.

From these diagrams and the Feynman rules coming from the effective action of the previous section, it is possible to obtain the differential cross section:

$$\frac{d\sigma(q\bar{q}\to g\pi\pi)}{dk^2dt} = \frac{4\alpha_s N}{3}\frac{(k^2-4M^2)^2}{184320f^8\pi^2\hat{s}^3tu}\sqrt{1-\frac{4M^2}{k^2}} \times(\hat{s}k^2+4tu)(2\hat{s}k^2+t^2+u^2), \quad (10)$$

where $\hat{s} \equiv (p_1 + p_2)^2$, $t \equiv (p_1 - q)^2$, $u \equiv (p_2 - q)^2$, and $k^2 \equiv (k_1 + k_2)^2$, p_1 and p_2 being the antiquark and quark four momenta, respectively, q the gluon four-momentum, and k_1 and k_2 the branon four momenta. We have assumed for the sake of simplicity that all the branons are degenerated with a common mass M and that all the quarks are massless. We have also neglected the effects of the top quark. In addition, we have the well-known relation $\hat{s} + t + u = k^2$. The contribution to the total cross section of the process $p\bar{p} \to g\pi\pi$ coming from this subprocess is given by

$$\sigma_{q\bar{q}}(p\bar{p}\to g\pi\pi) = \int_{x_{\min}}^1 dx \int_{y_{\min}}^1 dy \sum_q \bar{q}_{\bar{p}}(y;\hat{s}) q_p(x;\hat{s}) \times \int_{k^2_{\min}}^{k^2_{\max}} dk^2 \int_{t_{\min}}^{t_{\max}} dt \times \frac{d\sigma(q\bar{q}\to g\pi\pi)}{dk^2dt} + \cdots, \quad (11)$$

where $\bar{q}_{\bar{p}}(y;\hat{s})$ and $q_p(x;\hat{s})$ are the distribution functions of the antiquark inside the antiproton and of the quark of flavor q inside the proton, respectively, and x and y are the fractions of the proton and antiproton energy carried by the subprocess quark and antiquark. The different limits of the integrals can be written in terms of the cuts used to define the total cross section. For example, in order to be able to detect clearly the monojet, one must impose a minimal value for its transverse energy E_T and a pseudorapidity range given by $\eta_{\min}$ and $\eta_{\max}$. Then we have the limits $k^2_{\min} = 4M^2$, $k^2_{\max} = \hat{s}(1 - 2E_T/\sqrt{\hat{s}})$, and $t_{\min(\max)} = -(\hat{s} - k^2)[1 + \tanh(\eta_{\min(\max)})]/2$. On the other hand, $x_{\min} = s_{\min}/s$ and $y_{\min} = x_{\min}/x$, where s is the total center of mass energy squared of the process and

$$s_{\min} = 2E_T^2 + 4M^2 + 2E_T\sqrt{E_T^2 + 4M^2}. \quad (12)$$

In addition the dots in (11) represent the contribution of the case in which the quark comes from the antiproton and the antiquark comes from the proton.

The cross section of the subprocess $gg \to g\pi\pi$ is given by

$$\frac{d\sigma(gg\to g\pi\pi)}{dk^2dt} = \frac{\alpha_s N(k^2-4M^2)^2}{40960f^8\pi^2\hat{s}^3tu}\sqrt{1-\frac{4M^2}{k^2}}[\hat{s}^4+t^4 + u^4 - k^8 + 6k^4(\hat{s}^2+t^2+u^2) - 4k^2(\hat{s}^3+t^3+u^3)], \quad (13)$$

where the Mandelstam variables are defined as in the previous case, with p_1 and p_2 being the initial gluon four momenta, q the final gluon four momentum, and $k = k_1 + k_2$ the total branon four momentum. Then the con-

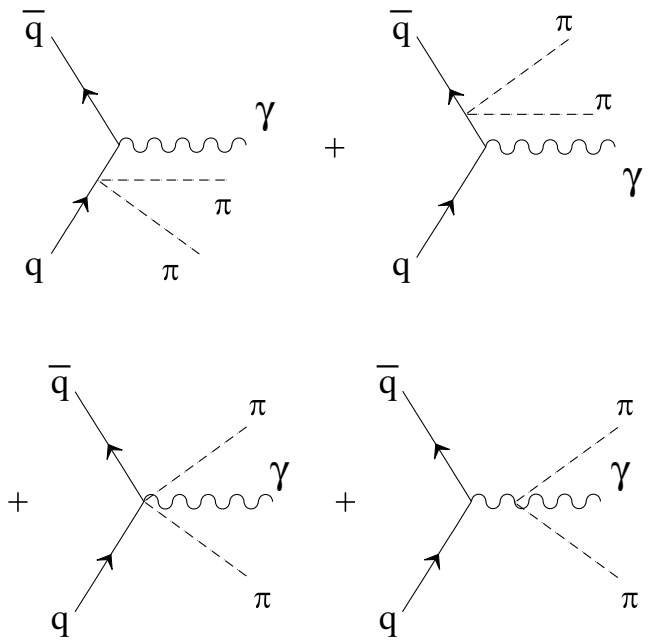

FIG. 4. Feynman diagrams associated with the $q\bar{q} \to \gamma\pi\pi$ subprocess.

tribution to the total cross section from the $p\bar{p} \to g\pi\pi$ reaction is

$$\sigma_{gg}(p\bar{p} \to g\pi\pi) = \int_{x_{\min}}^{1} dx \int_{y_{\min}}^{1} dy g(y;\hat{s}) g(x;\hat{s}) \times \int_{k^2_{\min}}^{k^2_{\max}} dk^2 \int_{t_{\min}}^{t_{\max}} dt \frac{d\sigma(gg \to g\pi\pi)}{dk^2 dt}. \quad (14)$$

Here $g(x;s)$ is the gluon distribution function of the (anti)proton, x and y are the fractions of the proton and antiproton energy carried by the initial gluons, and the integration limits remain the same. From the above equations, it is possible to compute the total cross section $\sigma(p\bar{p} \to g\pi\pi)$ in terms of the cut in the gluon (monojet) transverse energy E_T.

For the $qg \to q\pi\pi$ process, the cross section is given by

$$\frac{d\sigma(qg \to q\pi\pi)}{dk^2 dt} = -\frac{\alpha_s N}{2} \frac{(k^2 - 4M^2)^2}{184320 f^8 \pi^2 \hat{s}^3 tu} \sqrt{1 - \frac{4M^2}{k^2}} \times (uk^2 + 4t\hat{s})(2uk^2 + t^2 + \hat{s}^2), \quad (15)$$

with p_1 and p_2 being the quark and the gluon four momenta, respectively, q the final state quark four momentum, and k_1 and k_2 the branon four momenta. The Mandelstam variables are defined as in previous cases. The cross section for the conjugate process $\bar{q}g \to \bar{q}\pi\pi$ is exactly the same. Then the total cross section for the reaction $p\bar{p} \to q\pi\pi$ is

$$\sigma(p\bar{p} \to q\pi\pi) = \int_{x_{\min}}^{1} dx \int_{y_{\min}}^{1} dy \sum_q g(y;\hat{s}) q_p(x;\hat{s}) \times \int_{k^2_{\min}}^{k^2_{\max}} dk^2 \int_{t_{\min}}^{t_{\max}} dt \frac{d\sigma(qg \to q\pi\pi)}{dk^2 dt} + \cdots. \quad (16)$$

In this equation x and y are the fractions of the proton and antiproton energy carried by the subprocess quark and gluon. The different integration limits are defined as in the previous case in terms of the minimal transverse energy of the quark (monojet) E_T, and the dots refer to the case where the initial gluon is coming from the proton and the quark is coming from the antiproton. In addition, we have the contribution from the conjugate case where we take an antiquark from the proton and a gluon from the antiproton and conversely. This amounts just to a factor of 2.

From all the above equations, it is possible to compute the total cross section $\sigma(p\bar{p} \to J\pi\pi)$ in terms of the cut in the jet transverse energy E_T.

For the subprocess $q\bar{q} \to \gamma\pi\pi$, the cross section is given by

$$\frac{d\sigma(q\bar{q} \to \gamma\pi\pi)}{dk^2 dt} = \frac{Q_q^2 \alpha N (k^2 - 4M^2)^2}{184320 f^8 \pi^2 \hat{s}^3 tu} \sqrt{1 - \frac{4M^2}{k^2}} \times (\hat{s}k^2 + 4tu)(2\hat{s}k^2 + t^2 + u^2). \quad (17)$$

Here the notation is similar to the $q\bar{q} \to g\pi\pi$ case with the obvious differences in couplings, color, and charge factors. Thus,

$$\sigma(p\bar{p} \to \gamma\pi\pi) = \int_{x_{\min}}^{1} dx \int_{y_{\min}}^{1} dy \sum_q \bar{q}_{\bar{p}}(y;\hat{s}) q_p(x;\hat{s}) \times \int_{k^2_{\min}}^{k^2_{\max}} dk^2 \int_{t_{\min}}^{t_{\max}} dt \frac{d\sigma(q\bar{q} \to \gamma\pi\pi)}{dk^2 dt} + \cdots. \quad (18)$$

All the previous discussion about branon production in $p\bar{p}$ reactions can be easily translated to the pp case. The only point is to change the antiproton distribution functions of the different partons by the corresponding proton ones.

IV. ELECTRON(POSITRON)-PROTON COLLIDERS

For electron(positron)-proton colliders like HERA, the most interesting branon creating process is branon photoproduction, where a photon emitted by the electron(positron) interacts with a quark(antiquark) from the proton giving a quark (antiquark) and a branon pair. Thus, the experimental signature is again one monojet J plus missing energy and momentum. The relevant Feynman diagrams are shown in Fig. 5 and the corresponding differential cross section for the subprocess $\gamma q \to q\pi\pi$ is

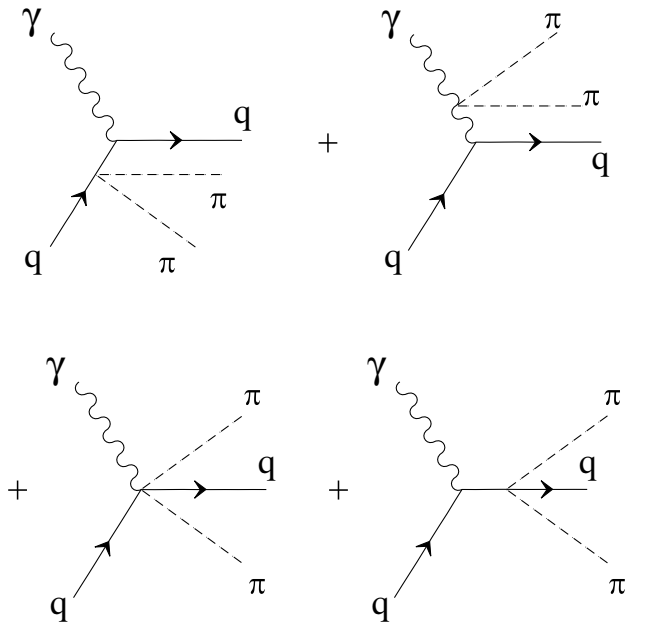

FIG. 5. Feynman diagrams associated with the $q\gamma \to q\pi\pi$ subprocess. The $\bar{q}\gamma \to \bar{q}\pi\pi$ subprocess has the same diagrams but changes the quark lines by the corresponding antiquark ones.

$$\frac{d\sigma(\gamma q \to q\pi\pi)}{dk^2 dt} = -\frac{3Q_q^2 \alpha N (k^2 - 4M^2)^2}{184320 f^8 \pi^2 \hat{s}^3 tu}\sqrt{1 - \frac{4M^2}{k^2}} \times (uk^2 + 4t\hat{s}^2)(2uk^2 + t^2 + \hat{s}^2), \tag{19}$$

where $\hat{s} = (p + q)^2$, $t = (p - k)^2$, and $u = (q - k)^2$, p being the photon, q the proton quark, q' the final quark, and k the total branon momenta, respectively. The total cross section for the process $e^{\pm} p \to q\pi\pi$ is given by

$$\sigma(e^{\pm} p \to q\pi\pi) = \int_{x_{\min}}^{1} dx \int_{y_{\min}}^{1} dy \sum_q F(y) q_p(x;\hat{s}) \times \int_{k^2_{\min}}^{k^2_{\max}} dk^2 \int_{t_{\min}}^{t_{\max}} dt \frac{d\sigma(\gamma q \to q\pi\pi)}{dk^2 dt}. \tag{20}$$

x and y are defined in this case as $q = xP_p$ and $P = yP_e$ with P_p and P_e being the proton and electron(positron) momenta, respectively. Thus, at high energies compared with the proton mass $\hat{s} = xys$, where $s = (P_e + P_p)^2$. The integral limits $y_{\min}$, $x_{\min}$, $k^2_{\min,\max}$, and $t_{\min,\max}$ are defined as in the proton-(anti)proton collider case.

The photon spectrum $F(y)$ can be obtained from the well-known Weizsäcker-Williams approximation [11]:

$$F(y) = \frac{\alpha}{2\pi y}[1 + (1 - y)^2] \log \frac{s'}{4m_e^2}, \tag{21}$$

with $s' = xs$ and m_e being the electron mass.

The cross section $\sigma(e^{\pm} p \to \bar{q}\pi\pi)$ can be obtained in a similar way. Then the total contribution to monojet plus missing energy and momentum production for large enough E_T coming from branons can be written as the sum of $\sigma(e^{\pm} p \to q\pi\pi)$ and $\sigma(e^{\pm} p \to \bar{q}\pi\pi)$.

V. RESULTS

By using the cross sections shown in the previous sections, it is possible to compute the expected number of branon pairs produced in the different hadron colliders in terms of the brane tension parameter f, the branon mass M, and the number of branons N. To this end we have used the distribution functions which can be found in [12]. The values of the electromagnetic and strong couplings have been taken at the electroweak boson masses, namely, $\alpha = 0.0781$ and $\alpha_s = 0.1171$. However, our final results do not depend too much on the precise value of these couplings. In fact, our main source of error is the use of an effective action to describe the SM particles and branon interactions since, in principle, this is only guaranteed for energies well below $4\pi f$.

As discussed in the introduction, our main goal in this work is to study the bounds that can be set on the f, M, and N parameters coming from hadron colliders. We will present all our limits at the 95% confidence level. In particular, for the electron(positron)-proton case, HERA is the most relevant experiment. In fact, the ZEUS collaboration has studied the jet production in charged current deep inelastic $e^+ p$ scattering. Its results are perfectly compatible with the SM background and therefore we can set some bounds on the branon production and, hence, on the f, M, and N parameters. These data were taken from 1995 to 2000 at a maximum CM energy of 318 GeV. The total integrated luminosity was 110.5 pb^{-1} and the cuts on the pseudorapidity and the transverse energy were $-1 \leq \eta \leq 2$ and $E_T \geq 14$ GeV (see [13] for more details). By using the same cuts with our cross sections for monojet plus a branon pair production, we find the bound $f > 16N^{1/8}$ GeV for massless branons. For a branon mass larger than 152 GeV, there are no restrictions on the f value because of kinematical reasons. For the intermediate M values, the bounds obtained can be seen in Fig. 6 where we have assumed $N = 1$. For other N values, one just has to take into account that the bound scales like $N^{-1/8}$ since all the cross sections are proportional to Nf^{-8}.

In the $p\bar{p}$ case, the most relevant experimental information so far is the one obtained at the Tevatron (Run I). The D0 detector has studied the monojet channel and CDF the single-photon one. As far as the number of events found in both cases is compatible with the SM background, we can set new bounds on the branon theory parameters. For light branons the most important bound comes from the D0 data. These data were taken from 1994 to 1996 at a CM energy of 1.8 TeV and correspond to an

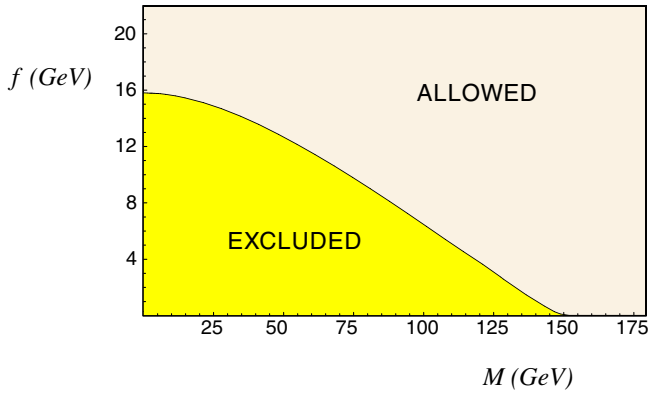

FIG. 6 (color online). Exclusion region at the 95% C.L. in the parameter space $f - M$ for $N = 1$ from ZEUS data on jet production.

integrated luminosity 78.8 ± 3.9 pb^{-1}. The cuts on the pseudorapidity and the transverse energy were $|\eta| \leq 1$ and $E_T \geq 150$ GeV (see [14] for the details of the analysis). The total number of monojets observed was 38 and the expected number from the SM plus cosmic ray events was 38 ± 9.6. By using our cross sections for monojet plus a branon pair production with these cuts, we get the bound $f > 157N^{1/8}$ GeV for light branons. The restrictions for f extend up to a branon mass of 822 GeV. For the intermediate M values the bounds obtained can be seen in Fig. 7 for $N = 1$.

In a similar way, we can use the CDF data on single-photon production. In this case the total luminosity collected was 87 ± 4 pb^{-1} and the pseudorapidity cut was $|\eta| \leq 1$. For the transverse photon energy several cuts were considered (for example, 55 GeV at the 75% efficiency). The total expected background for this process was 11.0 ± 2.2, without taking into account the QCD contribution (see [15] for the details of the analysis), and the number of events found was 11. Comparing this result with our computations for photon plus one branon pair production, we find the bound $f > 148N^{1/8}$ GeV for massless branons and no bound for M larger than 872 GeV. The bound obtained for the rest of the cases is shown also in Fig. 7.

In addition to this analysis corresponding to the Tevatron data (Run I), it is also interesting to make some estimation about the bounds that could be set from future experiments such as Tevatron (Run II) and the LHC. In the case of the Tevatron (Run II), which is already in progress, the main novelties are a CM energy which equals 1.96 TeV and an expected integrated luminosity $\mathcal{L}_{II}$ at the end of the run of about 200 pb^{-1}. The detectors are also improved so that the pseudorapidity cuts can be taken as $|\eta| \leq 3$ for D0 and $|\eta| \leq 3.6$ for CDF. This would result in a factor of $\sqrt{\mathcal{L}_{II}/\mathcal{L}_I}$ on the statistical significance when compared to Run I, with integrated luminosity $\mathcal{L}_I$, provided that the CM energy and the cuts were the same. For massless branons, the bound on f scales as the CM energy $E_{\mathrm{CM}}^{3/4}$. Even more important is the possibility of exploring higher branon masses, since the kinematical limit is given by $M_0 = \sqrt{E_{\mathrm{CM}}^2 - 2E_{\mathrm{CM}}E_T}/2$. In Fig. 8 we show the expected bounds from Run II in the $f - M$ plane, again for $N = 1$.

The LHC will produce pp collisions at a CM energy of 14 TeV and the integrated luminosity will be something about 10^5 pb^{-1}. In order to estimate the bounds on the f, M, and N parameters that will be possible to obtain at the LHC, we have proceeded in a similar way as in the Tevatron case, with the obvious changes in the distribution functions due to the fact that now we are dealing with pp instead of $p\bar{p}$ collisions. We have kept the same cuts except for the transverse energy which has been corrected in order to maintain the same proportion relative to the CM energy. Again the best bounds for f come

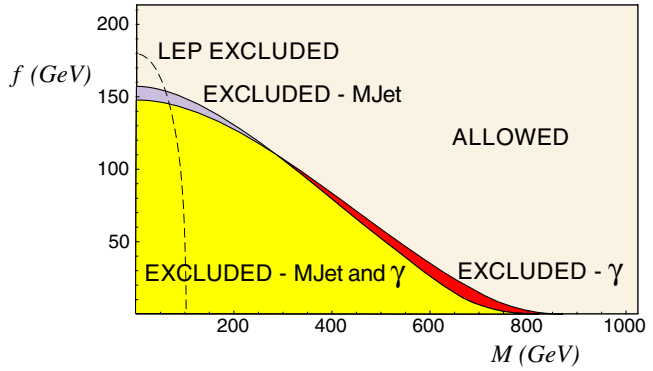

FIG. 7 (color online). Exclusion region $f - M$ at the 95% C.L. for $N = 1$ with D0 data in the monojet channel, and with CDF data in the single-photon channel. The dashed line corresponds to the LEP-II limits obtained by the L3 collaboration using single-photon data [8].

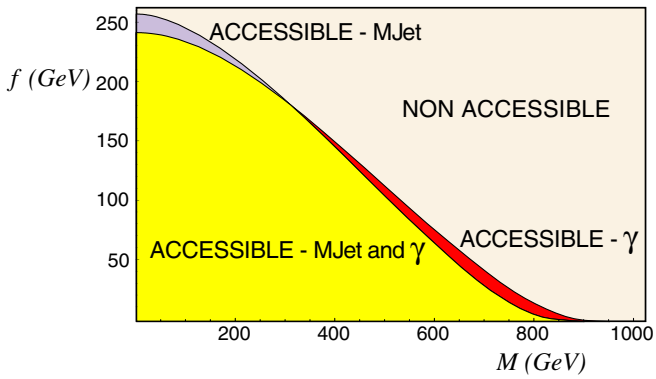

FIG. 8 (color online). Sensitivity estimation at the 95% C.L. for the second run of Tevatron in the parameter space $f - M$ for $N = 1$.

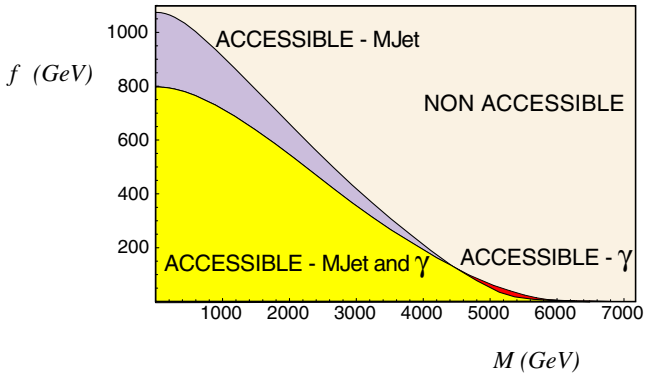

FIG. 9 (color online). Sensitivity estimation at the 95% C.L. for the LHC in the $f - M$ plane for $N = 1$.

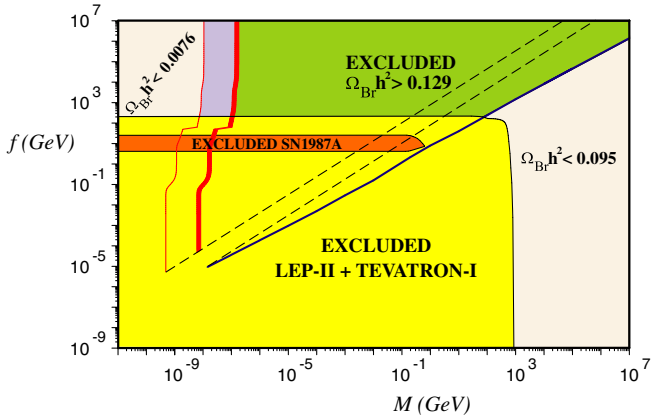

FIG. 10 (color online). Relic abundance in the $f - M$ plane for a model with one branon of mass: M. The two lines on the left correspond to the $\Omega_{Br}h^2 = 0.0076$ and $\Omega_{Br}h^2 = 0.129$–0.095 curves for hot-warm relics, whereas the right line corresponds to the latter limits for cold relics (see [10] for details). The lower area is excluded by single-photon processes at LEP-II [8] together with monojet signal at Tevatron-I. The astrophysical constraints are less restrictive and they mainly come from supernova cooling by branon emission [10].

from monojet production, which for $M = 0$ turns out to be $f > 1075N^{1/8}$ GeV. For low f, the best bound for M is given by the single-photon channel ($M_0 = 6781$ GeV). The LHC sensitivity for other values in the $f - M$ plane can be found in Fig. 9 for $N = 1$.

VI. CONCLUSIONS

In this work we have studied the flexible brane-world scenario, where the brane tension scale f is much smaller than the fundamental D-dimensional gravitational scale M_D. In this case, the relevant low-energy degrees of freedom are the SM particles and the brane fluctuations or branons. From the corresponding effective action, we have calculated the relevant cross sections for different branon searches in hadronic colliders. We have used the information coming from HERA and the first Tevatron run in order to get different exclusion plots on the branon mass M and the tension scale f plane for a given branon number N. Monojet production turns out to be the most efficient process for light branons, whereas the single-photon channel is the most important one for heavy branons.

We have also extended the analysis to future hadronic colliders. The corresponding sensitivity regions for the second Tevatron run and the LHC have also been plotted (see Table I for a summary of the analysis).

These analyses improve those already done for electron-positron colliders for heavy branons, whereas for light branons the results are similar [7–9]. The Tevatron (Run I) limit $M_0 = 872$ GeV can be compared to the analogous limit from LEP-II $M_0 = 103$ GeV [8]. According to the previous estimations, Tevatron Run II could also improve the bound $f_0 = 180$ GeV obtained by LEP-II. On the other hand, LHC could detect branons up

TABLE I. Summary of the main characteristics of the analysis performed for hadronic colliders. All the results are presented at the 95% C.L. We have studied two channels: the one marked with an upper index [1] is related to monojet production, whereas the single-photon is labeled with an upper index [2]. We considered four different experiments: HERA, the I and II Tevatron runs, and the LHC. Obviously, the data corresponding to the two last experiments are estimations, whereas the first two analyses have been performed with real data. $\sqrt{s}$ is the center of mass energy associated to the total process; $\mathcal{L}$ is the total integrated luminosity; E_T is the transverse energy cut; $\eta_{\mathrm{min,max}}$, the pseudorapidity limits; σ_0 is the estimation for the cross section sensitivity limit; f_0 is the bound in the brane tension scale for one massless branon ($N = 1$), and M_0 is the limit on the branon mass for $f = 0$.

Experiment	$\sqrt{s}$ (TeV)	$\mathcal{L}$ (pb^{-1})	E_T (GeV)	$\eta_{\mathrm{max,min}}$	σ_0 (GeV^{-2})	f_0 (GeV)	M_0 (GeV)
HERA[1]	0.318	110.5	14	-1, two	7.010^{-7}	16	152
Teva-I[1]	1.8	78	150	-1, one	6.310^{-10}	157	822
Teva-I[2]	1.8	87	55	-1.1, 1.1	1.310^{-10}	148	872
Teva-II[1]	1.96	10^3	150	-3, three	3.210^{-10}	256	902
Teva-II[2]	1.96	10^3	55	-3.6, 3.6	7.010^{-11}	240	952
LHC[1]	14	10^5	1000	-3, three	1.810^{-11}	1075	6481
LHC[2]	14	10^5	430	-3.6, 3.6	3.810^{-12}	797	6781

to a mass of several TeV ($M_0 = 6781$ GeV) improving even the compact linear collider prospects ($M_0 \simeq 2500$ GeV) [7].

The study of branons in colliders can be complemented with other bounds coming from astrophysics and cosmology (see Fig. 10). In fact, as shown in [10], the branon relic abundance can have cosmological consequences. Other issues related to branon phenomenology, such as their radiative corrections to the SM processes or their distinctive signatures at colliders with respect to the KK gravitons, will be analyzed elsewhere.

ACKNOWLEDGMENTS

We would like to thank J. Terrón, M. Vázquez, and M. Spiropulu for useful comments and experimental information. This work has been partially supported by the DGICYT (Spain) under Projects No. FPA2000-0956 and No. BFM2002-01003.

Note added.—After this paper was completed, we were informed by Spiropulu that the CDF collaboration had performed a monojet study [16] which could improve the bounds in a more detailed analysis.

[1] N. Arkani-Hamed, S. Dimopoulos, and G. Dvali, Phys. Lett. B **429**, 263 (1998); N. Arkani-Hamed, S. Dimopoulos, and G. Dvali, Phys. Rev. D **59**, 086004 (1999); I. Antoniadis *et al.*, Phys. Lett. B **436**, 257 (1998).

[2] A. Perez-Lorenzana, AIP Conf. Proc. **562**, 53 (2001); V. A. Rubakov, Phys. Usp. **44**, 871 (2001); Usp. Fiz. Nauk **171**, 913 (2001); Y. A. Kubyshin, hep-ph/0111027; C. Csaki, hep-ph/0404096.

[3] M. Bando *et al.*, Phys. Rev. Lett. **83**, 3601 (1999).

[4] R. Sundrum, Phys. Rev. D **59**, 085009 (1999); A. Dobado and A. L. Maroto, Nucl. Phys. B **592**, 203 (2001).

[5] J. A. R. Cembranos, A. Dobado, and A. L. Maroto, Phys. Rev. D **65**, 026005 (2002); J. A. R. Cembranos, A. Dobado, and A. L. Maroto, hep-ph/0107155.

[6] A. A. Andrianov *et al.*, J. High Energy Phys. 07 (2003) 063.

[7] J. Alcaraz *et al.*, Phys. Rev. D **67**, 075010 (2003); J. A. R. Cembranos, A. Dobado, and A. L. Maroto, AIP Conf. Proc. **670**, 235 (2003).

[8] L3 Collaboration, P. Achard *et al.*, Phys. Lett. B **597**, 145 (2004).

[9] P. Creminelli and A. Strumia, Nucl. Phys. B **596**, 125 (2001).

[10] J. A. R. Cembranos, A. Dobado, and A. L. Maroto, Phys. Rev. Lett. **90**, 241301 (2003); T. Kugo and K. Yoshioka, Nucl. Phys. B **594**, 301 (2001); J. A. R. Cembranos, A. Dobado, and A. L. Maroto, Phys. Rev. D **68**, 103505 (2003); A. L. Maroto, Phys. Rev. D **69**, 043509 (2004); J. A. R. Cembranos, A. Dobado, and A. L. Maroto, hep-ph/0307015; hep-ph/0402142; A. L. Maroto, Phys. Rev. D **69**, 101304 (2004);AMS Collaboration, AMS Internal Note 2003-08-02.

[11] C. von Weizsäcker, Z. Phys. **88**, 612 (1934); E. J. Williams, Phys. Rev. **45**, 729 (1934).

[12] A. D. Martin *et al.*, Eur. Phys. J. C **4**, 463 (1998); H. L. Lai *et al.*, Eur. Phys. J. C **12**, 375 (2000); , http://durpdg.dur.ac.uk.

[13] ZEUS Collaboration, S. Chekanov *et al.*, Eur. Phys. J. C **31**, 149 (2003); M. L. Vazquez, Doctoral thesis, Autonoma University, Madrid, 2002.

[14] D0 Collaboration, V. M. Abazov *et al.*, Phys. Rev. Lett. **90**, 251802 (2003).

[15] CDF Collaboration, D. Acosta *et al.*, Phys. Rev. Lett. **89**, 281801 (2002).

[16] CDF Collaboration, D. Acosta *et al.*, Phys. Rev. Lett. **92**, 121802 (2004).